Available online at www.sciencedirect.com
SCIENCE DIRECT®
ELSEVIER
Finite Elements in Analysis and Design 40 (2004) 1417–1427
FINITE ELEMENTS IN ANALYSIS AND DESIGN
www.elsevier.com/locate/finel

# Topology optimization of nonlinear structures

Daeyoon Jung, Hae Chang Gea*

*Department of Mechanical and Aerospace Engineering, Rutgers, The State University of New Jersey, Piscataway, NJ 08854, USA*

Received 3 April 2003; accepted 19 August 2003

**Abstract**

In this paper, topology optimization of both geometrically and materially nonlinear structure is studied using a general displacement functional as the objective function. In order to consider large deformation, effective stress and strain are expressed in terms of 2nd Piolar–Kirchhoff stress tensor and Green–Lagrange strain tensor, and constitutive equation is derived from the relation between the effective stress and strain. Sensitivity analysis of the general displacement functional is derived using the adjoint method. Numerical results of mean compliance design are compared under linear analysis, geometrical nonlinear analysis, material nonlinear analysis, and combined nonlinear analysis.


*Keywords:* Geometrical nonlinearity; Material nonlinearity; Topology optimization

## 1. Introduction

Since the introduction of topology optimization to the design of continuum structures [1], it has been successfully applied to many different types of structural design problems. Suzuki and Kikuchi [2] considered topology optimization of linear elastic plane structures for the stiffest design using the homogenization method. Duysinx and Bendsøe [3] extended the topology optimization techniques to the optimization of continuum structures with local stress constraints. Compliant mechanism design using topology optimization techniques has been studied extensively [4–7]. The optimal stiffener design of shell/plate structures with the small deformation was studied by Luo and Gea [8], Pedersen [9], Chen and Wu [10]. Gea and Fu [11] studied vibration problem using topology optimization to maximize eigenfrequencies with the assumption of linear elastic structural behavior.

* Corresponding author. Tel.: +1-732-445-0108.
*E-mail address:* gea@rci.rutgers.edu (H.C. Gea).

0168-874X/$ - see front matter © 2003 Elsevier B.V. All rights reserved.
doi:10.1016/j.finel.2003.08.011

An extensive literature survey can be found in Bendsøe [12]. Most of the works mentioned above are based on the assumption of small deformation during optimization process. But in some design applications such as energy absorbing structure and compliant mechanism, the assumption of small deformation is not valid any more. In order to get more realistic designs for the applications with large deformation, both geometrical and material nonlinearities must be considered.

When a structure undergoes sufficiently large deformation, the structure exhibits nonlinear behavior. This nonlinear behavior comes from two different sources: geometrical and material. The former requires the update of equilibrium and the latter results in the failure of linear material model. Sensitivity analysis of nonlinear analysis can be found in the monograph by Haug and Choi [13]. Buhl, et al. [14] studied topology optimization with geometrically nonlinearity and showed the solutions of linear analysis may differ from those of nonlinear analysis. Bruns et al. [15] and Gea, et al. [16] also found similar results from their studies. Pedersen et al. [17] studied compliant mechanism for maximizing output work and path generation by incorporating geometrical nonlinearity. Sigmund [5,6] applied topology optimization with geometrical nonlinearity to electrothermomechanical device with one or two materials. Burns et al. [18] demonstrated the snap-through of nonlinear elastic strcutures with topology optimization. A heuristic approach for energy absorption applications was presented by Soto [19].

Research works on topology optimization with material nonlinearity can also be found. Yuge and Kikuchi [20] optimized a frame structure under a plastic deformation using elastoplastic material model with the assumption of linear work-hardening. Bendsøe [21] applied a strain softening material to solve optimization problems of structure and material properties. Mayer et al. [22] applied topology optimization to crashworthiness problem using elastoplastic material model. Pedersen [23] developed a power-law nonlinear material model for rigidity based topology optimization. Maute et al. [24] used elastoplastic material model for the topology optimization of materially nonlinear structures and the material is assumed linear work-hardening elastoplastic. Jung and Gea [25] studied the effect of material nonlinearity using different material model on the compliant mechanism design generated by topology optimization approach. However, reports on topology optimization with both geometrical and material nonlinearities are still very limited.

In this paper, topology optimization of geometrically and materially nonlinear structure is studied simultaneously. In order to consider large deformation, effective stress and strain are expressed in terms of 2nd Piolar–Kirchhoff stress and Green–Lagrange strain tensor and constitutive equation is derived from the relation between effective stress and strain. Mean compliance is selected as an objective function and the sensitivity of general displacement functional is derived using the adjoint method. The optimization problem is formulated by using microstructure-based design domain method and solved iteratively using generalized convex approximation(GCA) ([26]). Numerical examples are presented and discussed to illustrate the difference between the combined nonlinear analysis and linear or geometrical-only/material-only analyses.

## 2. Analysis of nonlinear structure

In order to consider geometrical nonlinearity, the effective stress and strain are derived from 2nd Piola–Kirchhoff stress tensor and Green–Lagrange strain tensor [27]. A general relation between effective stress and strain is used to describe the material nonlinearity in this work. In this section,

constitutive equation combining both material nonlinearity and geometric nonlinearity is discussed and the linearized incremental analysis is presented.

### 2.1. Constitutive equation

To effectively analyze structures under large deformation, the effective stress and strain is expressed in terms of 2nd Piola–Kirchhoff stress tensor and the Green–Lagrange strain tensor. The effective strain is defined as

$$\varepsilon_{\mathrm{e}}^2 = \varepsilon_{ij} C_{ijkl}^0 \varepsilon_{kl}, \tag{1}$$

where $\varepsilon_{\mathrm{e}}$ denotes the effective strain, $\varepsilon_{ij}$ represents the Green–Lagrange strain tensor and $C_{ijkl}^0$ is a positive definite and dimensionless matrix. The nonlinear characteristics of material is modelled by a general relation between the effective stress and the effective strain is defined

$$\sigma_{\mathrm{e}} = K f(\varepsilon_{\mathrm{e}}), \tag{2}$$

where function $f(\varepsilon_{\mathrm{e}})$ is a general function representing the material characteristics and $K$ is a constant reference modulus of elasticity. For example, in the power-law material model, $f(\varepsilon_{\mathrm{e}})$ is in the form of $\varepsilon_{\mathrm{e}}^n$ with $n$ as the work-hardening exponent. Because the strain energy density, $u$ must be consistent regardless of the strain/stress types, we have the following relation:

$$u = \int_0^{\varepsilon_{ij}} S_{ij}\, \mathrm{d}\varepsilon_{ij} = \int_0^{\varepsilon_{\mathrm{e}}} \sigma_{\mathrm{e}}\, \mathrm{d}\varepsilon_{\mathrm{e}}, \tag{3}$$

where $S_{ij}$ represents 2nd Piola–Kirchhoff stress tensor. By taking the derivative of Eq. (1), we have $\varepsilon_{\mathrm{e}}\, \mathrm{d}\varepsilon_{\mathrm{e}} = \varepsilon_{ij} C_{ijkl}^0\, \mathrm{d}\varepsilon_{kl}$. Substituting the result into Eq. (3) and replacing $\sigma_{\mathrm{e}}$ with $K f(\varepsilon_{\mathrm{e}})$ from the Eq. (2), we have constitutive equation in the form of

$$S_{ij} = K f(\varepsilon_{\mathrm{e}})/\varepsilon_{\mathrm{e}} C_{ijkl}^0 \varepsilon_{kl} = K g(\varepsilon_{\mathrm{e}}) C_{ijkl}^0 \varepsilon_{kl}, \tag{4}$$

where $g(\varepsilon_{\mathrm{e}}) = f(\varepsilon_{\mathrm{e}})/\varepsilon_{\mathrm{e}}$. With the simple manipulation of Eq. (4), 2nd Piola–Kirchhoff stress tensor can be transformed into the scalar effective stress.

$$\sigma_{\mathrm{e}}^2 = S_{ij} {C_{ijkl}^0}^{-1} S_{kl}. \tag{5}$$

### 2.2. Linearized incremental analysis

When a structure constituted with materials described as Eq. (4) is subjected to body forces, $f_i^{\mathrm{B}}$, surface traction, $f_i^{\mathrm{S}}$ on the surface $S_{f_i}$ and displacement boundary condition, $S_{u_i}$, its responses are obtained by using constitutive equation, equilibrium equation, and strain–displacement relation. The equilibrium equation can be expressed with virtual displacement in the weak form

$$\int_V {}^{t+\Delta t} S_{ij}\, \delta\, {}^{t+\Delta t}\varepsilon_{ij}\, \mathrm{d}^{t+\Delta t} V = \int_V f_i^{\mathrm{B}}\, \delta\, {}^{t+\Delta t} u_i\, \mathrm{d}^{t+\Delta t} V + \int_S f_i^{\mathrm{S}}\, \delta\, {}^{t+\Delta t} u_i^{\mathrm{S}}\, \mathrm{d}^{t+\Delta t} S. \tag{6}$$

The Green–Lagrange strain tensor is defined as

$$\varepsilon_{ij} = \frac{1}{2}\left(\frac{\partial u_i}{\partial x_j} + \frac{\partial u_j}{\partial x_i} + \frac{\partial u_k}{\partial x_i}\frac{\partial u_k}{\partial x_j}\right). \tag{7}$$

The equilibrium equation (Eq. (7)) cannot be solved directly due to the nonlinearities in the constitutive equation and the strain–displacement relation. It is solved iteratively by using incrementally linearized equations. In the incremental analysis, responses of structure at $t+\Delta t$ state are calculated by adding the incremental responses occurred during the incremental configuration change to those of the current state, $t$ [27]. And responses at the configuration state $t$ can be obtained by incrementally accumulating responses from the initial state, 0, to the current state, $t$. When the change in displacement under incremental forces is assumed as $\Delta u_i$, incremental strain are obtained by replacing $u_i$ with $u_i + \Delta u_i$ in Eq. (7).

$${}^{t+\Delta t}\varepsilon_{ij} = {}^{t}\varepsilon_{ij} + \Delta\varepsilon_{ij}, \tag{8}$$

where the incremental strain, $\Delta\varepsilon_{ij}$, can be decomposed into its linear increment ($e_{ij}$) and nonlinear increment ($\eta_{ij}$) as follows:

$$\Delta\varepsilon_{ij} = e_{ij} + \eta_{ij},$$

$$e_{ij} = \frac{1}{2}\left(\frac{\partial\Delta u_i}{\partial x_j} + \frac{\partial\Delta u_j}{\partial x_i} + \frac{\partial\Delta u_k}{\partial x_i}\frac{\partial {}^{t}u_k}{\partial x_j} + \frac{\partial {}^{t}u_k}{\partial x_i}\frac{\partial\Delta u_k}{\partial x_j}\right), \tag{9}$$

$$\eta_{ij} = \frac{1}{2}\left(\frac{\partial\Delta u_j}{\partial x_i}\right)\left(\frac{\partial\Delta u_i}{\partial x_j}\right). \tag{10}$$

Similarly, stress state at state, $t+\Delta t$, can be obtained by adding incremental stress to stress at current state, $t$.

$${}^{t+\Delta t}S_{ij} = {}^{t}S_{ij} + \Delta S_{ij} = {}^{t}S_{ij} + \frac{\partial\, {}^{t}S_{ij}}{\partial\, {}^{t}\varepsilon_{kl}}\Delta\varepsilon_{kl} = {}^{t}S_{ij} + {}^{t}C^{\tan}_{ijkl}\Delta\varepsilon_{kl}. \tag{11}$$

Therefore, incremental stress can be expressed as $\Delta S_{ij} = {}^{t}C^{\tan}_{ijkl}\Delta\varepsilon_{kl}$. ${}^{t}C^{\tan}_{ijkl}$ is the tangent modulus tensor at the current strain state of ${}^{t}\varepsilon_{kl}$ and it can be computed by taking the derivative of the constitutive equation, Eq. (4), with respect to strain, $\varepsilon_{kl}$, as follows:

$$\begin{aligned} {}^{t}C^{\tan}_{ijkl} &= Kg(\varepsilon_e)C^0_{ijkl} + K\frac{1}{\varepsilon_e}\frac{\partial g(\varepsilon_e)}{\partial\varepsilon_e}C^0_{ijkl}\,{}^{t}\varepsilon_{kl}\frac{\partial\varepsilon_e}{\partial\, {}^{t}\varepsilon_{kl}}, \\ &= Kg(\varepsilon_e)C^0_{ijkl} + K\frac{1}{\varepsilon_e}\frac{\partial g(\varepsilon_e)}{\partial\varepsilon_e}C^0_{ijpq}\varepsilon_{pq}\varepsilon_{rs}C^0_{rskl}. \end{aligned} \tag{12}$$

The equilibrium equation is linearized by replacing ${}^{t+\Delta t}S_{ij}$ with Eq. (11) and $\delta^{t+\Delta t}\varepsilon_{ij}$ with $\delta e_{ij} + \delta\eta_{ij}$ because strain at state $t$ is a reference state during the incremental analysis. The multiplication of $\Delta S_{ij}$ and $\delta\eta_{ij}$ is assumed to be small. Therefore, the linearized form of equilibrium equation is as follows:

$$\int_{{}^{0}V}^{t} C^{\tan}_{ijkl}e_{kl}\delta e_{kl}\,\mathrm{d}^0V + \int_{{}^{0}V}^{t} S_{ij}\delta\eta_{ij}\,\mathrm{d}^0V = {}^{t+\Delta}R - \int_{{}^{0}V}^{t} S_{ij}\delta e_{ij}\,\mathrm{d}^0V, \tag{13}$$

where ${}^{t+\Delta t}R = \int_{t+\Delta t V} {}^{t+\Delta t} f_i^{\mathrm{B}} \delta u_i \, \mathrm{d}^{t+\Delta t} V + \int_{t+\Delta t S_f} {}^{t+\Delta t} f_i^{\mathrm{S}} \delta u_i^{\mathrm{S}} \, \mathrm{d}^{t+\Delta t} S$ is the virtual work of all external forces. The right-hand side of the above equation represents "out-of-balance virtual work" due to the linear approximation and the analysis should be repeated until the out-of balance term is less than the satisfactory level. The left-hand side of Eq. (13) represents virtual work expression of tangent structure corresponding to the current displacement and stress field.

## 3. Optimization problem

One of the most commonly used functionals in structural optimization is the displacement functional. Many examples of displacement functional can be found in engineering applications, such as the mean compliance for stiffness design, the regional strain energy for energy absorption design, and the Geometric Advantage (GA)/the Mechanical Advantage (MA) for compliant mechanism design. In this section, sensitivity analysis of a general displacement functional will be derived using the adjoint method. Consider a general displacement functional, $H$, as,

$$H = \int_V h(u_i, p) \, \mathrm{d}V, \tag{14}$$

where $u_i$ denotes the displacement field and $p$ represents the design variables. To derive the sensitivity of the displacement functional, we introduce a new functional, $H^*$, by including three additional terms to $H$: the strain–displacement relation, the constitutive equation of the nonlinear material model, and the equilibrium equation of the structure as

$$\begin{aligned} H^* = H &+ \int_V S_{ij}^{\mathrm{a}} \left( \varepsilon_{ij} - \frac{1}{2} \left( \frac{\partial u_i}{\partial x_j} + \frac{\partial u_j}{\partial x_i} + \frac{\partial u_k}{\partial x_i} \frac{\partial u_k}{\partial x_j} \right) \right) \mathrm{d}V \\ &+ \int_V \varepsilon_{ij}^{\mathrm{a}} (S_{ij} - Kg(\varepsilon_{\mathrm{e}}) C_{ijkl}^0 \varepsilon_{kl}) \, \mathrm{d}V + \int_V f_i^{\mathrm{B}} u_i^{\mathrm{a}} \, \mathrm{d}V + \int_V f_i^{\mathrm{S}} u_i^{\mathrm{S,a}} \, \mathrm{d}S \\ &- \frac{1}{2} \int_V S_{ij} \left( \frac{\partial u_i^{\mathrm{a}}}{\partial x_j} + \frac{\partial u_j^{\mathrm{a}}}{\partial x_i} + \frac{\partial u_k^{\mathrm{a}}}{\partial x_i} \frac{\partial u_k}{\partial x_j} + \frac{\partial u_k}{\partial x_i} \frac{\partial u_k^{\mathrm{a}}}{\partial x_j} \right) \mathrm{d}V, \end{aligned} \tag{15}$$

where $S_{ij}^{\mathrm{a}}$, $\varepsilon_{ij}^{\mathrm{a}}$ and $u_i^{\mathrm{a}}$ are the various states of the adjoint structure to be determined; $f_i^{\mathrm{B}}$ and $f_i^{\mathrm{S}}$ denote the body forces and surface traction, respectively. It is obvious that both the original functional, $H$ and the new functional, $H^*$, are identical. By taking the derivative of Eq. (15) with respect to the design variable $p$ and collecting the terms with $\partial S_{ij}/\partial p$ and $\partial \varepsilon_{ij}/\partial p$ from the results of the previous derivative, we have

$$\begin{aligned} \frac{\mathrm{d}H}{\mathrm{d}p} = &\int_V \frac{\partial h}{\partial p} \, \mathrm{d}V + \int_V \frac{\partial h}{\partial u} \frac{\partial u}{\partial p} \, \mathrm{d}V \\ &+ \int_V \frac{\partial S_{ij}}{\partial p} \left( \varepsilon_{ij}^{\mathrm{a}} - \frac{1}{2} \left( \frac{\partial u_i^{\mathrm{a}}}{\partial x_j} + \frac{\partial u_j^{\mathrm{a}}}{\partial x_i} + \frac{\partial u_k^{\mathrm{a}}}{\partial x_i} \frac{\partial u_k}{\partial x_j} + \frac{\partial u_k}{\partial x_i} \frac{\partial u_k^{\mathrm{a}}}{\partial x_j} \right) \right) \mathrm{d}V \\ &+ \int_V \frac{\partial \varepsilon_{ij}}{\partial p} \left( S_{ij}^{\mathrm{a}} - \left( Kg(\varepsilon_{\mathrm{e}}) C_{ijkl}^0 + K \frac{1}{\varepsilon_{\mathrm{e}}} \frac{\partial g(\varepsilon_{\mathrm{e}})}{\partial \varepsilon_{\mathrm{e}}} C_{ij\,pq}^0 \varepsilon_{pq} \varepsilon_{rs} C_{rskl}^0 \right) \varepsilon_{kl}^{\mathrm{a}} \right) \mathrm{d}V \end{aligned}$$

$$-\frac{1}{2}\int_V S_{ij}^{\mathrm{a}}\left(\frac{\partial}{\partial x_j}\left(\frac{\partial u_i}{\partial p}\right)+\frac{\partial}{\partial x_i}\left(\frac{\partial u_j}{\partial p}\right)+\frac{\partial}{\partial x_i}\left(\frac{\partial u_k}{\partial p}\right)\frac{\partial u_k}{\partial x_j}+\frac{\partial u_k}{\partial x_i}\frac{\partial}{\partial x_j}\left(\frac{\partial u_k}{\partial p}\right)\right)\mathrm{d}V$$

$$-\int_V \varepsilon_{ij}^{\mathrm{a}}\frac{\partial K}{\partial p}\,g(\varepsilon_{\mathrm{e}})\varepsilon_{kl}\,\mathrm{d}V-\frac{1}{2}\int_V S_{ij}\left(\frac{\partial u_k^{\mathrm{a}}}{\partial x_i}\frac{\partial}{\partial x_j}\left(\frac{\partial u_k}{\partial p}\right)+\frac{\partial}{\partial x_i}\left(\frac{\partial u_k}{\partial p}\right)\frac{\partial u_k^{\mathrm{a}}}{\partial x_j}\right)\mathrm{d}V. \tag{16}$$

In the above equation, two integral terms leading with $\partial S_{ij}/\partial p$ and $\partial\varepsilon_{ij}/\partial p$ and the terms with $\partial u_i/\partial p$ can be eliminated by defining the adjoint structure as follows:

$$\varepsilon_{ij}^{\mathrm{a}}=\frac{1}{2}\left(\frac{\partial u_i^{\mathrm{a}}}{\partial x_j}+\frac{\partial u_j^{\mathrm{a}}}{\partial x_i}+\frac{\partial u_k^{\mathrm{a}}}{\partial x_i}\frac{\partial u_k}{\partial x_j}+\frac{\partial u_k}{\partial x_i}\frac{\partial u_k^{\mathrm{a}}}{\partial x_j}\right), \tag{17}$$

$$S_{ij}^{\mathrm{a}}=K\left\{g(\varepsilon_{\mathrm{e}})C_{ijkl}^{0}+\frac{1}{\varepsilon_{\mathrm{e}}}\frac{\partial g(\varepsilon_{\mathrm{e}})}{\partial\varepsilon_{\mathrm{e}}}C_{ijpq}^{0}\varepsilon_{pq}\varepsilon_{rs}C_{rskl}^{0}\right\}\varepsilon_{kl}^{\mathrm{a}}, \tag{18}$$

$$\int_V\frac{\partial h}{\partial u_i}\frac{\partial u_i}{\partial p}\,\mathrm{d}V=\frac{1}{2}\int_V S_{ij}\left(\frac{\partial u_k^{\mathrm{a}}}{\partial x_i}\frac{\partial}{\partial x_j}\left(\frac{\partial u_k}{\partial p}\right)+\frac{\partial}{\partial x_i}\left(\frac{\partial u_k}{\partial p}\right)\frac{\partial u_k^{\mathrm{a}}}{\partial x_j}\right)\mathrm{d}V$$

$$+\frac{1}{2}\int_V S_{ij}^{\mathrm{a}}\left(\frac{\partial}{\partial x_j}\left(\frac{\partial u_i}{\partial p}\right)+\frac{\partial}{\partial x_i}\left(\frac{\partial u_j}{\partial p}\right)+\frac{\partial}{\partial x_i}\left(\frac{\partial u_k}{\partial p}\right)\frac{\partial u_k}{\partial x_j}\right.$$

$$\left.+\frac{\partial u_k}{\partial x_i}\frac{\partial}{\partial x_j}\left(\frac{\partial u_k}{\partial p}\right)\right)\mathrm{d}V. \tag{19}$$

One can find the term within brackets in the Eq. (18) is same as the $C_{ijkl}^{\tan}$ of Eq. (12). By replacing the term with $C_{ijkl}^{\tan}$ in Eq. (18) and assigning the sensitivity of $\partial u_i/\partial p$ as $\delta u_i$, Eqs. (18) and (20) can be re-written as

$$S_{ij}^{\mathrm{a}}=C_{ijkl}^{\tan}\varepsilon_{kl}^{\mathrm{a}}, \tag{20}$$

$$\int_V\frac{\partial h}{\partial u_i}\delta u_i\,\mathrm{d}V=\frac{1}{2}\int_V S_{ij}^{\mathrm{a}}\left(\frac{\partial\delta u_i}{\partial x_j}+\frac{\partial\delta u_j}{\partial x_i}+\frac{\partial\delta u_k}{\partial x_i}\left(\frac{\partial u_k}{\partial x_j}\right)+\frac{\partial u_k}{\partial x_i}\frac{\partial\delta u_k}{\partial x_j}\right)\mathrm{d}V$$

$$+\frac{1}{2}\int_V S_{ij}\left(\frac{\partial u_k^{\mathrm{a}}}{\partial x_i}\frac{\partial\delta u_k}{\partial x_j}+\frac{\partial\delta u_k}{\partial x_i}\left(\frac{\partial u_k^{\mathrm{a}}}{\partial x_i}\right)\right)\mathrm{d}V. \tag{21}$$

Here, the adjoint system was formally defined. The stiffness matrix of the adjoint structure is found to be the same as that of the deformed structure under the original loading, and load applied to the adjoint structure can be calculated from $\partial h/\partial u_i$. Therefore, the adjoint structure is tangent structure corresponding to the finally deformed structure under load $\partial h/\partial u_i$. Finally, the sensitivity of the general displacement functional, $H$, can be expressed as the following form:

$$\frac{\mathrm{d}H}{\mathrm{d}p}=\int_V\frac{\partial h}{\partial p}\,\mathrm{d}V-\int_V\varepsilon_{ij}^{\mathrm{a}}\frac{\partial K}{\partial p}\,g(\varepsilon_{\mathrm{e}})C_{ijkl}^{0}\varepsilon_{kl}\,\mathrm{d}V, \tag{22}$$

where $\varepsilon_{ij}^{\mathrm{a}}$ is the strain tensor of adjoint structure and can be obtained by linear analysis for the adjoint structure.

## 4. Numerical examples

In this section, the optimization problem is formulated as minimizing the mean compliance with a volume constraint. We will firstly study the effects on the optimal topology from different analysis methods and then study the effects of the applied load.

Although the minimum mean compliance design of nonlinear structures may not be the stiffest one, the mean compliance formulation is sufficient for our purpose of demonstrating the effect of geometrical and material nonlinearities on the optimal solution. The optimization problem can be expressed as:

$$\text{minimize } \Pi = \int_V f_i u_i \, \mathrm{d}V,$$

$$\text{subject to } \int_V \rho \, \mathrm{d}V \leqslant V_0, \tag{23}$$

where $V_0$ denotes the upper bound of the allowable material. By replacing $h(u_i, p)$ of Eq. (22) with $f_i u_i$, the sensitivity of the objective function is obtained as $\mathrm{d}\Pi/\mathrm{d}p = -\int_V \varepsilon^{\mathrm{a}}_{ij}(\partial K/\partial p) g(\varepsilon_{\mathrm{e}}) C^0_{ijkl} \varepsilon_{kl} \, \mathrm{d}V$. Once the sensitivity analysis is completed, the topology optimization problem is solved by a convex approximation method developed by Chickermane and Gea [10] iteratively.

### 4.1. Example 1

A long slander beam with 160 cm long and 20 cm high is fixed along both ends as shown in Fig. 1. A 30 N concentrated force is applied at the center of bottom edge. Four different analyses are used in topology optimization for comparison: (a) linear analysis, (b) materially nonlinear analysis, (c) geometrically nonlinear analysis, and (d) coupled materially and geometrically nonlinear analysis. For simplicity, the nonlinear material model is chosen as a power-law material with 0.5 as work hardening exponent. However, other nonlinear material model can be used without any alternation in the derivations. The applied force is large enough to produce some material nonlinearity in the highly strained areas. Young's modulus is 30 MPa and Poisson's ratio is 0.3. Twenty percent of the total design domain is used as the volume constraint.

The optimal designs from different analysis methods are presented in Fig. 2. The results from linear analysis and materially nonlinear analysis are almost identical. But they are completely different from those from geometrically nonlinear analysis and coupled nonlinear analysis.

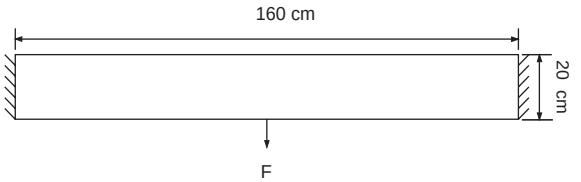


Fig. 1. Design domain for long slander beam.

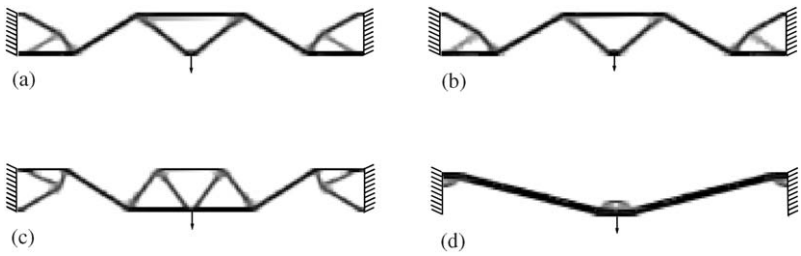


Fig. 2. Optimal designs from (a) linear analysis; (b) materially nonlinear analysis; (c) geometrically nonlinear analysis; (d) materially and geometrically nonlinear analysis.

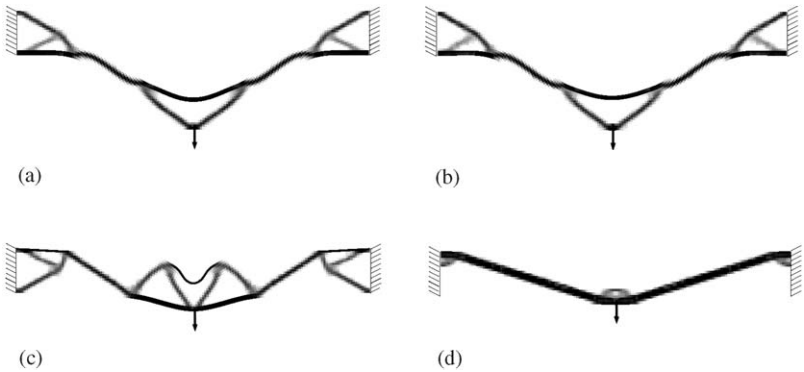


Fig. 3. Deformed shape of each design under combined nonlinear analysis of Fig. 2. (a) linear design (Mean compliance: 101.376 Nm); (b) materially nonlinear design (Mean compliance: 101.801 Nm); (c) geometrically nonlinear design (Mean compliance: 25.359); (d) materially and geometrically nonlinear design (Mean compliance: 12.924 Nm).

To further investigate these solutions, we applied coupled geometrically and materially nonlinear analysis to these four designs and the results are shown in Fig. 3. We found that the designs from linear analysis and materially nonlinear analysis fail to consider the penetration resulting from the large deformation. The same results were reported in the previous work by Gea and Luo [13]. However, even the optimal design from geometrically nonlinear analysis can avoid the penetration problem, it is still not as good as the optimal solution from the coupled analysis, 25.359 Nm vs. 12.924 Nm. The results show that topology optimization with coupled nonlinear analysis is a very useful tool for the applications like energy absorption structures and compliant mechanisms because these applications often use nonlinear material and require large deformation. However, nonlinear analysis is more computationally expensive than the linear one. Therefore, if applications do not involve in nonlinearity, topology with linear analysis would produce satisfactory results too.

### *4.2. Example 2*

In the second example, we will study the effects of applied force on the optimal designs. The same design domain as the first example is used. To make the comparison, the optimization is performed with the coupled nonlinear analysis. Four different magnitudes of force, 10, 15, 20 and 30 N are

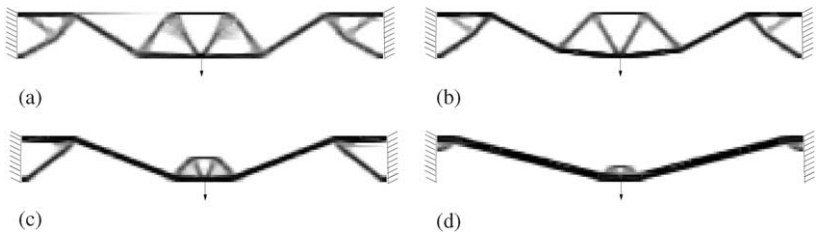


Fig. 4. Optimal designs based on combined nonlinear analysis under (a) 10 N; (b) 15 N; (c) 20 N; (d) 30 N.

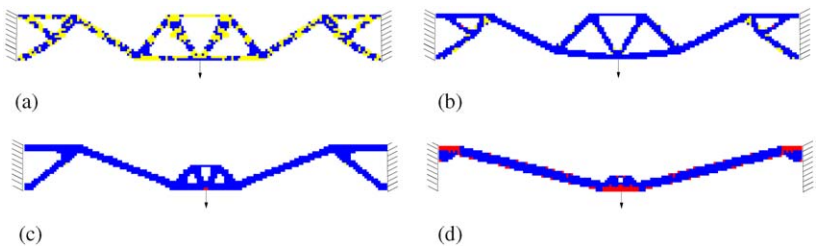


Fig. 5. Strain contour of each design in Fig. 4 under (a) 10 N; (b) 15 N; (c) 20 N; (d) 30 N.

applied to the center of bottom edge. The optimal solutions are shown in Fig. 4. We found that the optimal design under 10 N applied force using the coupled nonlinear analysis is very similar to the design from the geometrically nonlinear topology optimization in the previous example. When the applied force increases, the size of center structures decreases.

To understand the effects of applied load, the strain contours of each design are plotted in the Fig. 5. We only use three colors to represent different strain ranges: yellow implies low strain which is under the linear elastic limit, blue represents intermediate strain, and red is for highly strained region. When the applied load is 10 N, the strain level is not so high in most region of structure. Therefore, the material nonlinearity has not yet shown much and the optimal design is almost the same as the one considering geometrical nonlinearity only. While increasing the applied force to 15, 20, and 30 N, the strain level increases. The intermediate strain regions dominate the structure under 15 and 20 N; the highly strained areas show up in many places for 30 N applied force. When strain increases, the materially nonlinear effect starts to change the optimal configurations of the structure. This example further confirmed the importance of coupled nonlinear analysis in topology optimization with nonlinear materials, such as energy absorption designs.

## 5. Conclusion

In this paper, topology optimization with both geometrical and material nonlinearities was presented. To account for geometrical nonlinearity and material nonlinearity, constitutive equation was derived in terms of 2nd Piolar–Kirchhoff stress and Green–Lagrange strain tensors, and the nonlinear material is modelled by a general function between the effective stress and strain. The design sensitivity of displacement functionals was derived using the adjoint method. Numerical examples

showed that when the applications require nonlinear material and large deformation, the coupled nonlinear topology optimization should be used in order to produce the best design.

## References

[1] M.P. Bendsøe, N. Kikuchi, Generating optimal topologies in structural design using a homogenization method, Comput. Methods Appl. Mech. Eng. 71 (1988) 197–224.
[2] K. Suzuki, N. Kikuchi, A homogenization method for shape and topology optimization, Comput. Methods Appl. Mech. Eng. 93 (1991) 291–318.
[3] P. Duysinx, M.P. Bendsøe, Topology optimization of continuum structures with local stress constraints, Int. J. Numer. Methods Eng. 43 (1998) 1453–1478.
[4] G.K. Ananthasuresh, S. Kota, N. Kikuchi, Strategies for systematic synthesis of compliant MEMS, ASME Winter Annual Meeting, DSC-Vol. 55-2, 1994, pp. 677–686.
[5] O. Sigmund, Design of multiphysics actuators using topology optimization-Part I: one-material structures, Comput. Methods Appl. Mech. Eng. 190 (2001) 6577–6604.
[6] O. Sigmund, Design of multiphysics actuators using topology optimization-Part II: two-material structures, Comput. Methods Appl. Mech. Eng. 190 (2001) 6605–6627.
[7] S. Nishiwaki, M.I. Frecker, S. Min, N. Kikuchi, Topology optimization of compliant mechanisms using the homogenization method, Int. J. Numer. Methods Eng. 42 (1998) 535–559.
[8] J. Luo, H.C. Gea, A systematic topology optimization approach for optimal stiffener design, Struct. Optim. 16 (4) (1998) 280–288.
[9] N.L. Pedersen, Maximization of eigenvalues using topology optimization, Struct. Multidiscip. Optim. 20 (2000) 2–11.
[10] T.-Y. Chen, S.-C. Wu, Multiobjective optimal topology design of structures, Comput. Mech. 21 (1998) 483–494.
[11] H.C. Gea, Y. Fu, Optimal 3D stiffener design with frequency considerations, Adv. Eng. softwares 28 (1997) 525–531.
[12] M.P. Bendsøe, Optimization of Structural Topology, Shape, and Material, Springer, New York, 1995.
[13] E.J. Haug, K.K. Choi, Methods of Engineering Mathematics, Prentice-Hall, Englewood Cliffs, NJ, 1993.
[14] T. Buhl, C.B.W. Pedersen, O. Sigmund, Stiffness design of geometrically nonlinear structures using topology optimization, Struct. Multidiscip. Optim. 19 (2000) 93–104.
[15] T.E. Bruns, D.A. Tortorelli, Topology optimization of non-linear elastic structures and compliant mechanisms, Comput. Methods Appl. Mech. Eng. 190 (2001) 3443–3459.
[16] H.C. Gea, J. Luo, Topology optimization of structures with geometrical nonlinearities, Comput. Struct. 79 (2001) 1977–1985.
[17] C.B.W. Pedersen, T. Buhl, O. Sigmund, Topology synthesis of large-displacement compliant mechanisms, Int. J. Numer. Methods Eng. 50 (2001) 2683–2705.
[18] T.E. Bruns, O. Sigmund, D.A. Tortorelli, Numerical methods for topology optimization of nonlinear elastic structures that exhibit snap-through, Int. J. Numer. Methods Eng. 55 (10) (2002) 1215–1237.
[19] C.A. Soto, Optimal structural topology design for energy absorption: heuristic approach, ASME DETC 2001/DAC-21126.
[20] K. Yuge, N. Kikuchi, Optimization of a frame structure subjected to a plastic deformation, Struct. Optim. 10 (1995) 197–208.
[21] M.P. Bendsøe, J.M. Guedes, S. Plaxton, J.E. Taylor, Optimization of structure and material properties for solids composed of softening material, Int. J. Solids Struct. 33 (12) (1996) 1799–1813.
[22] R.R. Mayer, N. Kikuchi, R.A. Scott, Application of topological optimization techniques to structural crashworthiness, Int. J. Numer. Methods Eng. 39 (1996) 1383–1403.
[23] P. Pedersen, Some general optimal design results using anisotropic, power law nonlinear elasticity, Struct. Optim. 15 (1998) 73–80.
[24] K. Maute, S. Schwarz, E. Ramm, Adaptive topology optimization of elastoplastic structures, Struct. Optim. 15 (1998) 81–91.

[25] D. Jung, H.C. Gea, Compliant mechanism design with non-linear materials using topology optimization, Proceedings of the 2002 ASME Design Engineering Technical Conferences, Montreal, Canada, 2002, DETC2002/DAC-34150.
[26] H. Chickermane, H.C. Gea, Structural optimization using a new local approximation method, Int. J. Numer. Methods Eng. 39 (5) (1996) 829–846.
[27] K.J. Bathe, Finite Element Procedures, Prentice-Hall, Englewood Cliffs, NJ, 1996.